Insulin Resistance in Striated Muscle-specific Integrin Receptor β1-deficient Mice*

Haihong Zong[‡], Claire C. Bastie[‡], Jun Xu[§], Reinhard Fassler[¶], Kevin P. Campbell[‖], Irwin J. Kurland[§], and Jeffrey E. Pessin[‡1]

From the [‡]Departments of Medicine and Molecular Pharmacology, Albert Einstein College of Medicine, Bronx, New York 10461, [§]Department of Medicine, Stony Brook University, Stony Brook, New York 11794, [¶]Max Planck Institute for Biochemistry, Department of Molecular Medicine, Am Klopferspitz 18, 82152 Martinsried, Germany, and [‖]Howard Hughes Medical Institute, Departments of Molecular Physiology and Biophysics, Neurology, and Internal Medicine, Carver College of Medicine, The University of Iowa, Iowa City, Iowa 52242

Integrin receptor plays key roles in mediating both inside-out and outside-in signaling between cells and the extracellular matrix. We have observed that the tissue-specific loss of the integrin β1 subunit in striated muscle results in a near complete loss of integrin β1 subunit protein expression concomitant with a loss of talin and to a lesser extent, a reduction in F-actin content. Muscle-specific integrin β1-deficient mice had no significant difference in food intake, weight gain, fasting glucose, and insulin levels with their littermate controls. However, dynamic analysis of glucose homeostasis using euglycemic- hyperinsulinemic clamps demonstrated a 44 and 48% reduction of insulin-stimulated glucose infusion rate and glucose clearance, respectively. The whole body insulin resistance resulted from a specific inhibition of skeletal muscle glucose uptake and glycogen synthesis without any significant effect on the insulin suppression of hepatic glucose output or insulin-stimulated glucose uptake in adipose tissue. The reduction in skeletal muscle insulin responsiveness occurred without any change in GLUT4 protein expression levels but was associated with an impairment of the insulin-stimulated protein kinase B/Akt serine 473 phosphorylation but not threonine 308. The inhibition of insulin-stimulated serine 473 phosphorylation occurred concomitantly with a decrease in integrin-linked kinase expression but with no change in the mTOR·Rictor·LST8 complex (mTORC2). These data demonstrate an *in vivo* crucial role of integrin β1 signaling events in mediating cross-talk to that of insulin action.

Integrin receptors are a large family of integral membrane proteins composed of a single α and β subunit assembled into a heterodimeric complex. There are 19 α and 8 β mammalian subunit isoforms that combine to form 25 distinct α,β heterodimeric receptors (1–5). These receptors play multiple critical roles in conveying extracellular signals to intracellular responses (outside-in signaling) as well as altering extracellular matrix interactions based upon intracellular changes (inside-

out signaling). Despite the large overall number of integrin receptor complexes, skeletal muscle integrin receptors are limited to seven α subunit subtypes (α1, α3, α4, α5, α6, α7, and αν subunits), all associated with the β1 integrin subunit (6, 7).

Several studies have suggested an important cross-talk between extracellular matrix and insulin signaling. For example, engagement of β1 subunit containing integrin receptors was observed to increase insulin-stimulated insulin receptor substrate (IRS)[2] phosphorylation, IRS-associated phosphatidylinositol 3-kinase, and activation of protein kinase B/Akt (8–11). Integrin receptor regulation of focal adhesion kinase was reported to modulate insulin stimulation of glycogen synthesis, glucose transport, and cytoskeleton organization in cultured hepatocytes and myoblasts (12, 13). Similarly, the integrin-linked kinase (ILK) was suggested to function as one of several potential upstream kinases that phosphorylate and activate Akt (14–18). In this regard small interfering RNA gene silencing of ILK in fibroblasts and conditional ILK gene knockouts in macrophages resulted in a near complete inhibition of insulin-stimulated Akt serine 473 (Ser-473) phosphorylation concomitant with an inhibition of Akt activity and phosphorylation of Akt downstream targets (19). However, a complex composed of mTOR·Rictor·LST8 (termed mTORC2) has been identified in several other studies as the Akt Ser-473 kinase (20, 21). In addition to Ser-473, Akt protein kinase activation also requires phosphorylation on threonine 308 Thr-30 by phosphoinositide-dependent protein kinase, PDK1 (22–24).

In vivo, skeletal muscle is the primary tissue responsible for postprandial (insulin-stimulated) glucose disposal that results from the activation of signaling pathways leading to the translocation of the insulin-responsive glucose transporter, GLUT4, from intracellular sites to the cell surface membranes (25, 26). Dysregulation of any step of this process in skeletal muscle results in a state of insulin resistance, thereby predisposing an individual for the development of diabetes (27–33). Although studies described above have utilized a variety of tissue culture cell systems to address the potential involvement of integrin receptor signaling in insulin action, to date there has not been

[2] The abbreviations used are: IRS, insulin receptor substrate; ILK, integrin-linked kinase; MCK, muscle creatine kinase; Itgβ1, integrin β1; KO, knockout; EU, euglycemic-hyperinsulinemic; PDK, phosphoinositide-dependent protein kinase; PI 3-kinase, phosphatidylinositol 3-kinase; GLUT4, glucose transporter isoform 4; GSK, glycogen synthase kinase.

any investigation of integrin function on insulin action or glucose homeostasis *in vivo*. To address this issue, we have taken advantage of Cre-LoxP technology to inactivate the β1 integrin receptor subunit gene in striated muscle. We have observed that muscle creatine kinase-specific integrin β1 knock-out (MCKItgβ1 KO) mice display a reduction of insulin-stimulated glucose infusion rate and glucose clearance. The impairment of insulin-stimulated skeletal muscle glucose uptake and glycogen synthesis resulted from a decrease in Akt Ser-473 phosphorylation concomitant with a marked reduction in ILK expression. Together, these data demonstrate an important cross-talk between integrin receptor function and insulin action and suggests that ILK may function as an Akt Ser-473 kinase in skeletal muscle.

EXPERIMENTAL PROCEDURES

Muscle-specific β1 Integrin Subunit Knock-out Mice—The floxed β1 integrin subunit (Itgβ1) mice were generated as previously described (34). To obtain striated muscle-specific knockouts, the floxed Itgβ1 mice were mated with the MCK-Cre recombinase transgenic mice (35). All the mice strains used in this study were backcrossed 6–9 generations into the C57Bl6/J strain. Genotyping were performed by PCR using genomic DNA isolated from the tails of 3–4-week-old mice. The primers (5′-TGATGAGGTTCGCAAGAACC-3′ and 5′-CCATGAGTGAACGAACCTGG-3′) for identifying carriers of the Cre-recombinase transgenic were used under the following conditions: 1 cycle of 94 °C for 5 min, 35 cycles of 94 °C for 1 min, 55 °C for 1 min, and 72 °C for 1 min followed by 1 cycle of 72 °C for 10 min. The primers for the floxed Itgβ1 genotyping (5′-AGGTGCCCTTCCCTCTAGA-3′ and 5′-GTGAAGTA-GGTGAAAGGTAAC) were used under the following conditions: 1 cycle of 94 °C for 2 min, 35 cycles of 94 °C for 1 min, 58 °C for 1 min, and 72 °C for 1 min followed by 1 cycle of 72 °C for 10 min. Mice were housed in a temperature-controlled environment with a 12-h light/12-h dark cycle and provided a standard chow diet with free access to food and water. Food intake and weights were determined daily, and all studies were performed on 14-week-old male mice. All animal protocols were performed in accordance with Stony Brook University Institutional Animal Care and Use Committee approval.

Plasma Analysis and Immunoblotting—Fasting blood samples were collected by tail bleeding after a 14-h fast. Glucose was measured using a glucose oxidase method on a Beckman glucose analyzer 2 (Beckman Instruments Inc., Fullerton, CA). Insulin levels were determined by enzyme-linked immunosorbent assay (Mercodia, Uppsala, Sweden). For acute insulin stimulation, the mice were fasted for 14 h and given an intraperitoneal injection with 1 unit/kg human recombinant insulin (Lilly). Ten minutes later the animals were anesthetized with pentobarbital sodium (50 mg/kg), and tissue samples were collected and immediately frozen at −80 °C.

Tissues isolated from both EU clamps and acute insulin stimulation were homogenized in ice-cold lysis buffer (50 mM Tris, pH 7.5, 150 mM NaCl, 1% Triton X-100, 1 mM EDTA, 1 mM phenylmethylsulfonyl fluoride, 0.25% sodium deoxycholate, 1 mM NaF, 1 mM Na$_3$VO$_4$, and 2 mM Na$_4$P$_2$O$_7$) containing a protease inhibitor mixture (Roche Diagnostics). The resultant lysates were centrifuged at 16,000 × *g* for 60 min at 4 °C, and protein concentrations were quantified using the BCA (bicinchoninic acid) protein assays (Pierce). The protein samples (30 μg) were separated on a 4–12% gradient SDS-PAGE gel and transferred to nitrocellulose membranes using a semidry electroblotter (Owl Separation System, Portsmouth, NH). Membranes were immunoblotted with β1 integrin monoclonal antibody (BD Pharmingen), GLUT4 polyclonal antibody (East Acres Biologicals Inc.), phospho-Ser-473, and phospho-Thr-308 Akt monoclonal antibodies, pan-protein kinase B /Akt polyclonal antibody, phospho-Ser-9-GSK3β, total GSK3β, phospho-Thr-642-AS160, total AS160 (Cell Signaling Technology, Inc.), ILK and talin monoclonal antibodies (Sigma), and α-dystroglycan antibody as previously described (36). Phospho-IRS1 and p110 association was determined by PY20 (BD Biosciences) and p110 (R&D Systems) immunoblotting of IRS1 immunoprecipitates (BD Biosciences). Quantification of all immunoblots was performed using NIH IMAGE software.

In Vivo Assessment of Insulin Action and Glucose Metabolism— Four days before the experiment, the mice were anesthetized with ketamine (100 mg/kg) and xylazine (10 mg/kg), and an indwelling catheter was introduced in the left internal jugular vein. The catheters were externalized through an incision in the skin flap behind the head, and the mice were returned to individual cages after the surgery. The mice were fully recovered from the surgery before the *in vivo* experiments, as reflected by their reaching preoperative weight. After an overnight fast, EU clamps were conducted in conscious mice as previously described (37). The 2-h EU clamp was conducted with a prime-continuous infusion of human insulin (2.5 milliunits/kg/min) and a variable infusion of 20% glucose to maintain glucose at ∼110 mg/dl. Insulin-stimulated whole body glucose metabolism was estimated using a prime continuous infusion of [3-³H]glucose (10 μCi bolus, 0.1 μCi/min; PerkinElmer Life Sciences). To determine the rate of basal glucose turnover, [3-³H]glucose (0.05 μCi/min) was infused for 2 h (basal period) before starting the EU clamp, and a blood sample was taken at the end of this basal period. To assess insulin-stimulated tissue-specific glucose uptake, 2-deoxy-D-[1-¹⁴C]glucose (PerkinElmer Life Sciences) was administered as a bolus (10 μCi) 75 min after the start of the clamp. Blood samples were taken at 80, 85, 90, 100, 110, and 120 min after the start of the EU clamp. To estimate basal muscle glucose uptake, 2-deoxy-D-[1-¹⁴C]glucose was infused with isotonic saline. All infusions were performed using microdialysis pumps (CMA/Microdialysis). At the end of the EU clamp, animals were euthanized with pentobarbital sodium (50 mg/kg), and different muscle groups, adipose tissue, heart, and liver were rapidly dissected and frozen at −80 °C for analysis.

During the clamp plasma glucose was monitored using 10 μl of plasma by glucose analyzer 2. For the determination of plasma [3-³H]glucose and 2-deoxy-D-[1-¹⁴C]glucose concentrations, plasma was deproteinized with ZnSO$_4$ and Ba(OH)$_2$, dried to remove ³H$_2$O, resuspended in water, and counted in scintillation fluid (Ultima Gold; Packard Instrument Co.). The plasma concentration of ³H$_2$O was determined by the difference between ³H counts without and with drying. For the determination of tissue 2-deoxy-D-[1-¹⁴C]glucose (2-DG)-6-phos-

phate (2-DG-6-P) content, tissue samples were homogenized, and the supernatants were subjected to an ion-exchange column to separate 2-DG-6-P from 2-DG, as described previously (38). The radioactivity of ^{3}H in tissue glycogen was determined by digesting tissue samples in KOH and precipitating glycogen with ethanol as previously described (37). Muscle glycogen synthesis was calculated as muscle [^{3}H]glycogen content divided by the area under the plasma [^{3}H]glucose-specific activity profile. Muscle glycolysis was estimated as the difference between muscle glucose uptake and muscle glycogen synthesis.

Activity and Exercise Capacity—Spontaneous locomoter activity of control Itgβ1$^{flox/flox}$ and MCKItgβ1 KO mice was determined by quantifying the number of beam breaks in *xy* axis of an Oxymax open-circuit indirect calorimetry system (Columbus Instruments, Columbus, OH). During the first 48 h of the experiment, animals were allowed free access to food and water. After 48 h, animals were still allowed free access to water, but they were not fed in the evening for 12 h (from 7 p.m. to 7 a.m.) and then re-fed for 24 h (7 a.m. to 7 a.m.). At the end of the experiment, the animals underwent an 8-h fast (7 a.m. to 3 p.m.). The locomotor activity was monitored by the number of beam breaks and was averaged and expressed as counts/h.

Running capacity was determined as described by Koch and Britton (39). Briefly, the MCKItgβ1 KO and Itgβ1$^{flox/flox}$ mice were acclimatized to a treadmill (Columbus Instruments) by running at 10 m/min for 15 min over 3 consecutive days. On the fourth day, groups of mice were run at 10 m/min on a 0° grade or 10 m/min on a 15° grade incline.

Immunofluorescence Microscopy—After an overnight fast (14 h), the mice were euthanized. The tissues were removed and embedded in optimal cutting temperature compound. The frozen tissue cross-sections (10 μm) were blocked with 3% bovine serum albumin in phosphate-buffered saline for 60 min at room temperature. Primary antibodies were used at the following dilutions: β1 integrin polyclonal antibody (1:100) and talin antibody (1:50). Fluorescently conjugated secondary antibodies (1:100, Jackson ImmunoResearch Laboratories) were added to the sections for 30 min at room temperature. Filamentous (F-) actin was visualized by incubation of the fixed tissue with phalloidin-fluorescein isothiocyanate (1:1000) for 30 min. After extensive washes with phosphate-buffered saline, the slides were mounted with Vectashield Mounting Medium (Vector Laboratories). The slides were observed with confocal fluorescent microscopy (model LSM510; Carl Zeiss MicroImaging, Inc.).

Statistical Analysis—Results are represented as the means ± S.E. Statistical significance was determined using an unpaired two-tailed Student's *t* test, with $p < 0.05$ considered significant.

RESULTS

Generation of Muscle-specific β1 Integrin Knock-out Mice—To investigate the selective function of the β1 integrin subunit on insulin action and glucose homeostasis, we generated a muscle-specific-deficient Itgβ1 mouse by crossing mice carrying a "floxed" allele of β1 integrin (Itgβ1) in which loxP sites were introduced flanking exon 2 of the entire mouse β1 integrin gene (40, 41) with transgenic mice carrying the MCK-promoter driving Cre-recombinase (35). Breeding of Itgβ1$^{flox/+}$ and MCK-
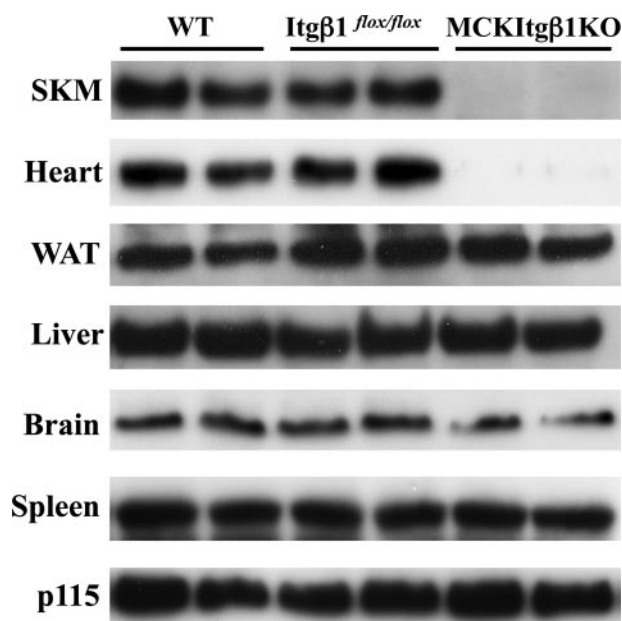
FIGURE 1. **MCK-Cre targeted disruption of the floxed β1 integrin receptor subunit gene results in skeletal muscle-specific knock-out.** Fourteen-week-old wild type (*WT*), Itgβ1$^{flox/flox}$, and littermate MCKItgβ1 KO mice in duplicate were fasted for 14 h. Tissues were harvested, and protein extracts from gastrocnemius skeletal muscle (*SKM*), heart, white adipose tissue (*WAT*), liver, brain, and spleen were then subjected to immunoblot analysis with the β1 integrin subunit-specific antibody. These are representative immunoblots independently performed with $n = 6$ to 10 mice for each strain.

TABLE 1
Physical parameters of MCKItgβ1 KO mice
Loss of integrin β1 expression in skeletal muscle of MCKItgβ1 KO mice at 14 weeks old does not affect food intake, weight, and fasting glucose and insulin levels.

|	Wild type	Itgβp1$^{flox/flox}$	MCKItgβ1KO
Food intake (g/day)	3.19 ± 0.8	3.21 ± 0.6	3.16 ± 0.74
Weight (g)	23.8 ± 1.3	24.9 ± 1.5	22.7 ± 1.19
Fasting glucose (mg/dl)	118.6 ± 9.8	112.6 ± 9.8	105 ± 9.9
Fasting insulin (milliunits/liter)	12.95 ± 1.6	12.75 ± 1.1	13.08 ± 0.76

Cre$^{+/-}$ mice resulted in double heterozygous animals that were then bred with Itgβ1$^{flox/+}$ mice to obtain Itgβ1$^{flox/flox}$:MCK-Cre offspring; that is, mice with a disruption of β1 integrin specifically in striated muscle (MCKItgβ1 KO). Offspring from these crosses resulted in the expected frequency of 12.5% for a trait requiring two independent loci, demonstrating the absence of embryonic lethality. To verify the extent of Itgβ1 recombination, we examined various tissues in two independent MCK-Cre-crossed mice by immunoblotting. These data demonstrated an almost complete loss of β1 integrin protein expression in skeletal and cardiac muscle with essentially wild type levels of protein expression in all the other tissues examined (Fig. 1). The p115 Golgi protein was used a protein loading control. General phenotypic characteristics of the MCKItgβ1 KO mice demonstrated that up to 14 weeks of age, there was no significant difference in overall body weight, food intake, fasting plasma glucose, and insulin concentrations compared with control Itgβ1$^{flox/flox}$ and wild type mice (Table 1).

Loss of Integrin β1 Expression in Skeletal Muscle Is Associated with Reduced Expression Levels of Talin and Actin Disorganization—Morphological examination of control skeletal muscle by confocal immunofluorescence microscopy dem-
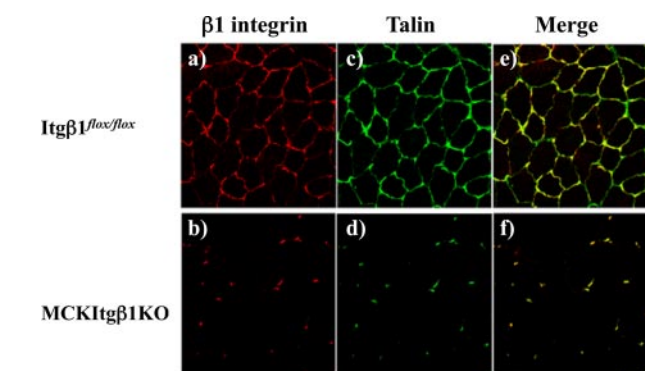
FIGURE 2. **Loss of β1 integrin receptor subunit expression results in a concomitant reduction in talin expression.** Skeletal muscle (gastrocnemius) was isolated from 14-week-old Itgβ1$^{flox/flox}$ and littermate MCKItgβ1 KO mice. The muscle was embedded, sectioned, and subjected to immunofluorescence analysis for β1 integrin subunit (*panels a and b*) and talin (*panels c and d*) expression. The merged images are shown in *panels e and f*.
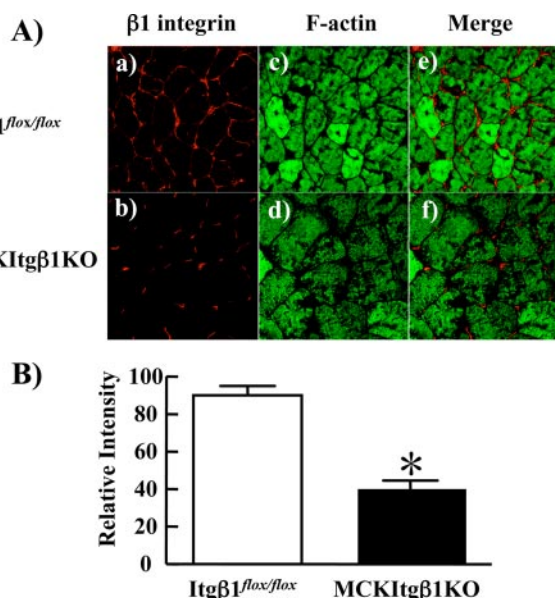
FIGURE 3. **Loss of β1 integrin receptor subunit expression results in a partial reduction and disorganization of F-actin filaments.** *A*, gastrocnemius muscle was isolated from 14-week-old Itgβ1$^{flox/flox}$ and littermate MCKItgβ1 KO mice. Sections were subjected to immunofluorescence analysis for β1 integrin expression (*panels a and b*) and F-actin (phalloidin-fluorescein isothiocyanate staining) levels (*panels c and d*). The merged images are shown in *panels e and f. B*, quantification of F-actin levels was determined by fluorescent intensity. $n = 6–10$ independent experiments. *, $p < 0.05$.

onstrated the presence of the integrin β1 subunit in the sarcolemma membrane (Fig. 2, *panel a*). As expected, there was a dramatic loss of integrin β1 expression in skeletal muscle of the MCKItgβ1 KO mice (Fig. 2, *panel b*). A concomitant loss of expression of the integrin β1 interacting protein talin was also observed in skeletal muscles of MCKItgβ1 KO mice (Fig. 2, *panels c and d*). Because β1 integrin receptors associate with the actin cytoskeleton via talin, we next investigated F-actin expression using phalloidin-fluorescein isothiocyanate staining (Fig. 3A, *panels a–f*). Concomitant with the reduction in talin there was reduced expression (52%) of F-actin in skeletal muscle of the MCKItgβ1 KO mice (Fig. 3B). The reduction in both talin and F-actin in skeletal muscle of the MCKItgβ1 KO mice occurred without a significant change in α-dystroglycan expression (data not shown).

Because there was significant morphological disorganization of muscle actin structure, we assessed muscle function by first assessing spontaneous motor activity (Fig. 4A). Over the first 48-h period, the mice were allowed to eat *ad libitum*, and there was no significant difference in activity during either the 12-h dark or 12-h light cycle. Similarly, locomotor activity was essentially identical when the animals were fasted either during the dark cycle or during the light cycle.

To examine the ability of the mice to respond to a greater demand of motor activity, we next determined the exercise tolerance of the MCKItgβ1 KO mice (Fig. 4B). The control Itgβ1$^{flox/flox}$ and the MCKItgβ1 KO mice were run on a level treadmill (0° degree) at 10 m/min. Over the 25-min challenge the mice tested were able to maintain this pace, and no significant differences between the Itgβ1$^{flox/flox}$ control and MCKItgβ1 KO mice were observed. In contrast, on a 15° grade incline, on average the MCKItgβ1 KO mice could only run for 12 min, whereas the control mice were able to maintain this pace for more than 20 min.

MCKItgβ1 KO Mice Display Insulin Resistance Due to Decreased Muscle Glucose Metabolism—To investigate the consequences of the muscle-specific ablation of the integrin β1 subunit on whole body glucose homeostasis and tissue-specific insulin action, we next examined changes in glucose and insulin levels during an intraperitoneal glucose tolerance test (Fig. 5). As reported in Table 1, there was no significant difference in the fasting plasma glucose levels between the controls and the KO mice. However the MCKItgβ1 KO mice displayed a trend toward impaired glucose tolerance that was significant at 120 min after glucose injection (Fig. 5A). Similarly, the fasting insulin levels were also not different compared with controls, but during the intraperitoneal glucose tolerance test the insulin levels were significantly elevated in the MCKItgβ1 KO mice (Fig. 5B). These data suggest that the MCKItgβ1 KO mice display peripheral tissue insulin resistance that is compensated for by increased beta cell insulin secretion to maintain euglycemia.

To more directly determine whether these mice are in fact insulin-resistant, we next performed a 2-h EU clamp in conscious MCKItgβ1 KO and Itgβ1$^{flox/flox}$ mice. No differences in plasma glucose or insulin levels were observed in either the basal or during the euglycemic-hyperinsulinemic clamp state (Fig. 6, *A* and *B*). However during the EU clamp, the rate of glucose infusion needed to maintain euglycemia increased rapidly in the control mice and reached a steady state. In contrast, the glucose infusion rate in response to insulin was reduced by 44% in the MCKItgβ1 KO mice compared with the control Itgβ1$^{flox/flox}$ mice (0.20 ± 0.03 *versus* 0.36 ± 0.02 mmol/kg/min) (Fig. 7A). Although there was no significant difference in glucose clearance between the MCKItgβ1 KO and control mice in the basal state, insulin-stimulated glucose clearance was significant decrease by 48% in the MCKItgβ1 KO mice (70.5 ± 5.6 *versus* 36.8 ± 9.4 ml/kg/min) (Fig. 7B). These data directly demonstrate the presence of insulin resistance in the MCKItgβ1 KO.

Insulin resistance can result from either decreased glucose uptake in peripheral tissue and/or enhanced hepatic glucose production. To assess tissue-specific insulin action, [3-³H]glucose and 2-deoxy-D-[1-¹⁴C]glucose infusion was performed
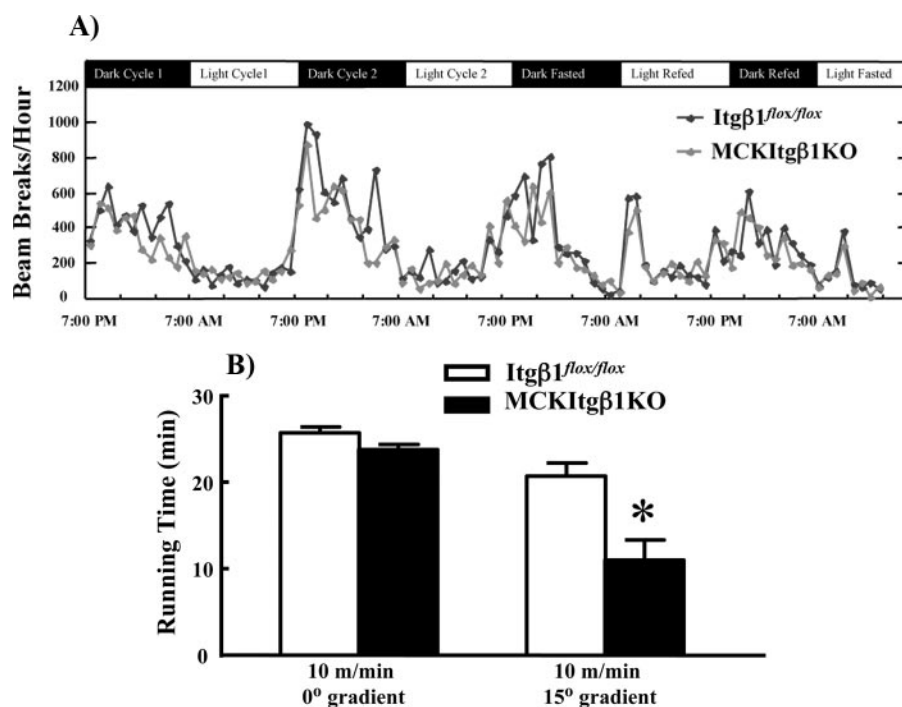
FIGURE 4. **Loss of β1 integrin receptor subunit expression has no effect on spontaneous locomotor activity but reduces exercise tolerance.** *A*, 14-week-old MCKItgβ1 KO (*n* = 4) and littermate control Itgβ1*flox/flox* mice (*n* = 4) were placed into Oxymax open-circuit indirect calorimetry system, and the number of XY beam breaks was collected over a 4-day period. During the first 2 days, the mice were allowed full access to food during both the light and dark cycles. After 48 h, the mice were fasted in the dark cycle and allowed to re-feed during the light cycle. At 72 h the mice were then allowed to re-feed during the dark cycle and fasted for 8 h during the light cycle. *B*, the wild type and MCKItgβ1 KO mice were placed on a treadmill and challenge to run at 10 m/min on a 0° or 15° grade incline for up to 25 min. The data indicate the amount of time that the mice were able to continually run. These data represent the means ± S.E. from 6–10 individual mice per group. $p <$ 0.005. Itgβ1*flox/flox* (*open boxes*) and MCKItgβ1KO (*filled boxes*).
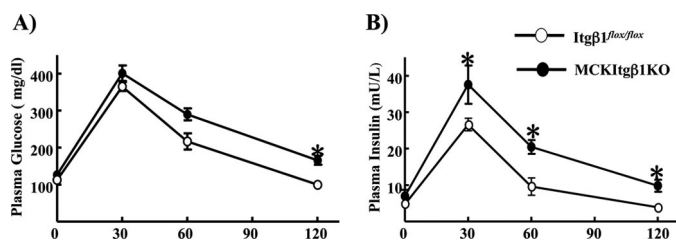
FIGURE 5. **MCKItgβ1 KO mice display a modestly impaired glucose tolerance due to compensatory increases in insulin secretion.** 14-Week-old MCKItgβ1 KO and littermate control Itgβ1*flox/flox* mice were fasted for 14 h and injected intraperitoneally with 1 g/kg D-glucose in isotonic saline. Blood (5–10 μl) was collected from the tail before and 30, 60, and 120 min after the injection. The changes in blood glucose (*A*) and insulin (*B*) levels were determined and represent the means ± S.E. from five individual mice per group. *, $p <$ 0.05. *Open circles*, Itgβ1*flox/flox*; *filled circles*, MCKItgβ1KO.

during the EU clamp. In the basal state, muscle-specific glucose uptake was not statistically different between control and MCKItgβ1 KO mice in mixed gastrocnemius (*Mixed Gastroc*), white gastrocnemius (*White Gastroc*), soleus, and cardiac muscles (Fig. 8*A*). In contrast, all these muscles displayed significant decreases in insulin-stimulated glucose uptake in the MCK-Itgβ1 KO (mixed gastrocnemius, 0.21 ± 0.06 *versus* 0.41 ± 0.06; white gastrocnemius, 0.14 ± 0.01 *versus* 0.26 ± 0.01; soleus, 0.75 ± 0.02 *versus* 1.18 ± 0.08; cardiac, 2.56 ± 0.28 *versus* 6.71 ± 0.44 compared with the control Itgβ1*flox/flox* mice (Fig. 8*B*). As controls, insulin-stimulated glucose uptake into adipose tissue was not significantly different between the control

Itgβ1*flox/flox* mice and the MCK-Itgβ1 KO mice (Fig. 9*A*). Similarly, insulin suppression of liver glucose output was also identical in the Itgβ1*flox/flox* mice and the MCK-Itgβ1 KO mice (Fig. 9*B*). Consistent with this impairment of insulin-stimulated glucose uptake in skeletal muscle, there was a concomitant 45% reduction in insulin-stimulated glycogen synthesis in the gastrocnemius of the MCKItgβ1 KO mice (Fig. 10). Although there was an apparent reduction in skeletal muscle glycolysis, this did not reach statistical significance. In any case, these abnormalities of insulin action in skeletal muscle glucose transport and glycogen synthesis activity suggest a common upstream defect in insulin signaling resulting in an impairment of skeletal muscle glucose uptake.

Insulin Signaling Is Impaired in MCKItgβ1 KO Mice—Several studies have demonstrated that insulin-stimulated glucose uptake depends on the translocation of intracellular stored GLUT4 proteins to muscle cell surface membranes (sarcolemma and t-tubule). This translocation process requires the activation of the Type IA phosphatidylinositol (PI) 3-kinase resulting in the activation of Akt via phosphorylation on Ser-473 and Thr-308 (42, 43). As expected, in the control Itgβ1*flox/flox* mice, insulin injection increased Akt phosphorylation on Ser-473 with no change in the total Akt content (Fig. 11*A*). Although the expression level of Akt was unchanged in the MCKItgβ1 KO mice, insulin-stimulated Akt Ser-473 phosphorylation was substantially reduced compared with the control Itgβ1*flox/flox* mice (0.4 ± 0.02 *versus* 0.5 ± 0.01 and 0.4 ± 0.001 *versus* 1.3 ± 0.02 in the Itgβ1*flox/flox*) (Fig. 11*B*). In contrast, insulin-stimulated Thr-308 phosphorylation was unaffected in the MCKItgβ1 KO mice (Fig. 11, *A* and *B*). The inability of insulin to stimulate Ser-473 Akt phosphorylation was also recapitulated at the end of the EU clamp that is equivalent to the insulin-stimulated state (Fig. 11*C*). That is, after the clamp the total level of skeletal muscle Akt protein was unchanged, but insulin-stimulated Akt Ser-473 phosphorylation was markedly reduced in the MCKItgβ1 KO mice compared with the Itgβ1*flox/flox* control mice. Although the total levels of GLUT4 and Akt proteins were relatively unchanged, the loss of β1 integrin expression, however, resulted a marked reduction in the protein expression levels of the ILK protein (Fig. 11*C*).

To determine whether the reduction in insulin-stimulated AKT Ser-473 phosphorylation occurred due to a defect in IRS signaling, we examined IRS1 tyrosine phosphorylation and IRS1 association with the p110 PI 3-kinase catalytic subunit

☐ Itgβ1*flox/flox*   ■ MCKItgβ1KO
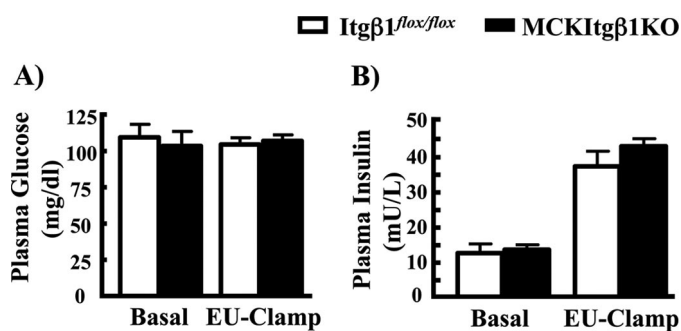
FIGURE 6. **Plasma glucose and insulin levels during the euglycemic-hyperinsulinemic clamp.** Plasma glucose (*A*) and plasma insulin (*B*) levels during basal and the last 30 min of EU clamp (2.5 milliunits/kg/min insulin infusion with glucose levels maintained at ∼110 mg/dl). *Open boxes*, Itgβ1*flox/flox*; *filled boxes*, MCKItgβ1KO. These data represent the means ± S.E. from eight individual mice per group.
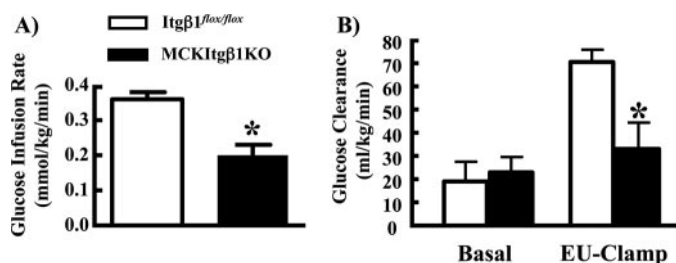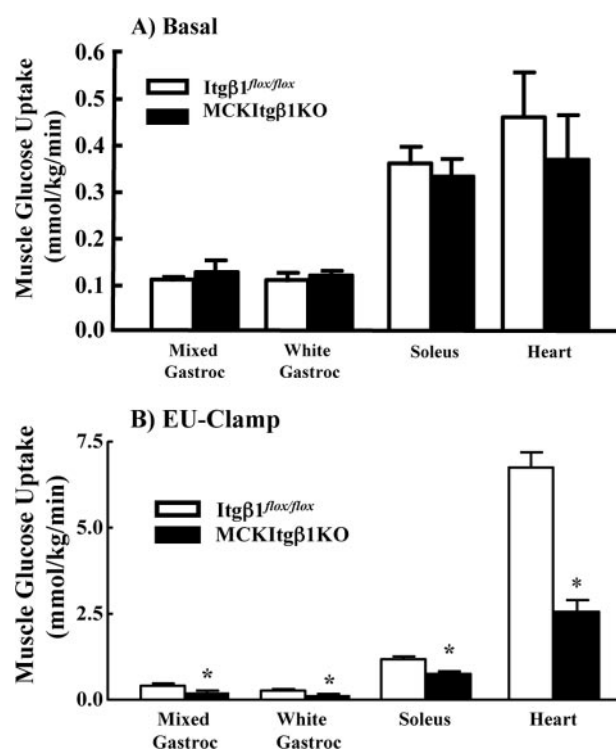

FIGURE 7. **Loss of skeletal muscle *β*1 integrin receptor subunit expression results in a decreased rate of insulin-stimulated glucose infusion rate and glucose clearance.** *A*, EU clamps were used to assess whole body insulin sensitivity by determining the glucose infusion rate required to maintain euglycemia into control Itgβ1*flox/flox* (*open boxes*) and MCKItgβ1KO (*filled boxes*) mice. *B*, glucose clearance was determined as [3-³H]glucose-specific activity trace infusion rate and weight of mice in the basal or EU clamp state. These data represent the means ± S.E. from 7–10 individual mice per group. *, $p < 0.05$.

(Fig. 12). The insulin-stimulated tyrosine phosphorylation of IRS1 was not significantly different between skeletal muscle of the control Itgβ1*flox/flox* and MCKItgβ1 KO mice (Fig. 12, *A* and *B*). Similarly, there was no significant difference in the insulin-stimulated association of IRS1 with the p110 catalytic subunit of the PI 3-kinase (Fig. 12, *A* and *C*). As expected, the reduction of Ser-473 Akt phosphorylation resulted in a marked inhibition of Akt-dependent downstream signaling, exemplified by the reduction in AS160 and GSK3β phosphorylation (Fig. 12, *D–G*).

To confirm the reduction in ILK expression in mice that were not subjected to the EU clamp procedure, we performed confocal fluorescent microscopy of skeletal muscle sections obtained from Itgβ1*flox/flox* and MCKItgβ1 KO mice (Fig. 13, *A* and *B*). In addition, we subjected total skeletal muscle tissue extracts to ILK immunoblotting (Fig. 13, *C* and *D*). These data confirmed the marked loss of ILK protein expression in the MCKItgβ1 KO mice compared with the control Itgβ1*flox/flox* mice. The reduction in ILK expression was in marked contrast to the expression levels of the mTORC2 complex, in which the expression levels of mTOR, Rictor, and LST8 were completely unaffected (Fig. 13*E*).

Taken together these data demonstrate that the loss of β1 integrin expression has multiple effects including impaired muscle insulin sensitivity and decreased glucose uptake that correlates with a reduced ability to activate Akt. Although Akt

FIGURE 8. **Loss of skeletal muscle *β*1 integrin receptor subunit expression results in a reduction of insulin-stimulated glucose uptake in skeletal muscle.** Basal (*A*) and insulin-stimulated glucose (*B*) uptake into several skeletal muscle tissues (mixed gastrocnemius (*Gastroc*), white gastrocnemius, soleus, and cardiac (Heart) muscles) were determined by 2-deoxy-D-[1-¹⁴C]glucose injection during the last 35 min of saline (*Basal*) or insulin infusion during the EU clamp. These data represent the means ± S.E. from five individual mice per group. *, $p < 0.05$. Itgβ1*flox/flox* mice (*open boxes*) and MCKItgβ1KO mice (*filled boxes*).
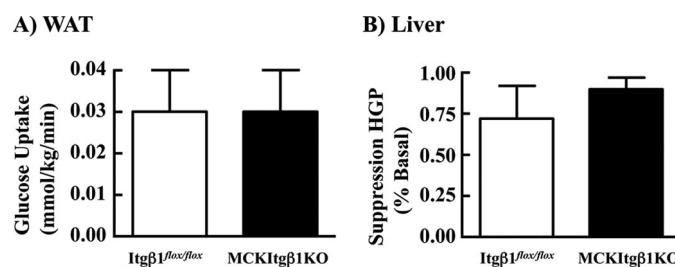
FIGURE 9. **Loss of skeletal muscle *β*1 integrin subunit expression has no effect on liver or adipose glucose metabolism.** Glucose uptake into adipose tissue (*WAT*) (*A*) and insulin (*B*) suppression of hepatic glucose output (*HGP, Liver*) was determined during the EU clamp by infusion of 2-deoxy-D-[1-¹⁴C]glucose or [3-³H]glucose infusion into control Itgβ1*flox/flox* (*open boxes*) and MCKItgβ1 KO (*filled boxes*) mice. These data represent the means ± S.E. from five individual mice per group. *, $p < 0.05$. Itgβ1*flox/flox* mice (*open boxes*) and MCKItgβ1KO mice (*filled boxes*).

and GLUT4 protein levels appear to be relatively normal, there is a marked reduction in ILK expression that may reflect a requirement for ILK function in the regulation of Akt phosphorylation on Ser-473 in skeletal muscle.

DISCUSSION

Post-prandial hyperglycemia in type II diabetes mellitus primarily results from reduced skeletal muscle glucose clearance from the circulation due to decreased in insulin-stimulated glucose uptake (26, 28, 44–46). It is well established that *in vivo* glucose transport into skeletal muscle is the rate-limiting step
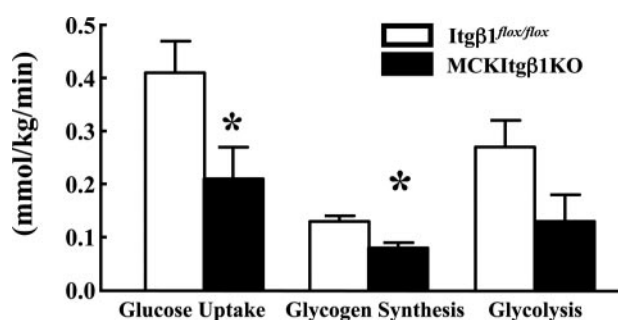
in glucose clearance, and impaired peripheral tissue insulin sensitivity results from a defect in this process (47, 48). Although the levels of GLUT4 protein are unaffected in states of insulin resistance, there is a marked impairment in the ability of insulin to induce its translocation from intracellular storage sites to the cell surface membrane (48). At the cellular level, multiple studies have suggested that insulin resistance involves decreases in insulin receptor-tyrosine kinase activity, IRS tyrosine phosphorylation, and/or activation of PI 3-kinase activity (25–28, 49). Other defects reported in muscle from obese and type 2 diabetic muscle include decreases in insulin-stimulated PKCλ/ξ activities as well as reduction in AS160 phosphorylation (30–32, 50, 51). Although the precise signaling pathways controlling GLUT4 translocation, particularly in skeletal mus-

FIGURE 10. **Loss of skeletal muscle β1 integrin receptor subunit expression results in reduced insulin-stimulated skeletal muscle glucose metabolism.** The amount of glucose transport (*Glucose Uptake*) glucose conversion to glycogen (*Glycogen Synthesis*) and metabolism to glucose 6-phosphate (*Glycolysis*) in gastrocnemius skeletal muscle of control Itgβ1$^{flox/flox}$ (*open boxes*) and MCKItgβ1KO (*filled boxes*) mice was determined during the EU clamp by infusion of [3-^{3}H]glucose infusion and 2-deoxy-D-[1-^{14}C]glucose as described under "Experimental Procedures." These data represent the means $\pm$ S.E. from five individual mice per group. *, $p < 0.05$. *Open boxes*, Itgβ1$^{flox/flox}$ mice; *filled boxes*, MCKItgβ1KO mice.

cle, have not been completely resolved, it is generally accepted that Akt activation is central to this process (42).
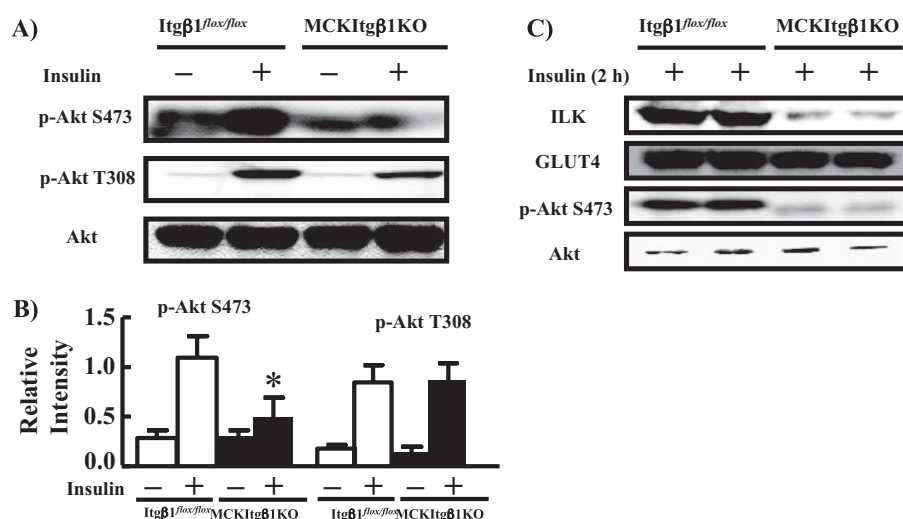
In this regard multiple studies have demonstrate that integrin receptor signaling plays important roles in integrating extracellular matrix and growth factor function on PI 3-kinase and Akt activities in multiple cell types (52–54). In particular, studies in isolated primary cell cultures and tissue-cultured cell lines have suggested a role for integrin receptor signaling in modulating insulin action (55). For example, cross linking of integrin β1 on the surface of isolated rat adipocytes with a β1 antibody or the addition of fibronectin enhanced insulin-stimulated IRS tyrosine phosphorylation, IRS-associated PI 3-kinase activity, and Akt activation (8).

To address the potential role of integrin β1 signaling in the modulation of insulin action *in vivo*, we generate striated muscle-specific knock-out mice, as the conventional whole body integrin β1 knock-out is embryonic lethal (34). In addition, it was reported that skeletal muscle knock-out of integrin β1 was lethal at birth due to respiratory failure resulting from an early loss of myoblast fusion and assembly of sarcomeres (7). The loss of integrin β1 expression can result in the impairment of heart function with cardiac failure occurring later in life but was not apparent at the age of mice that we have studied (56, 57). We have not observed any lethality, early muscle fusion or contraction defects in our striated muscle integrin β1 knock-out mice. However, we did observe a reduction in filamentous actin organization that may account for the decrease in exercise tolerance. Alternatively, it is also possible that a subtle cardiac dysfunction could account for the reduced exercise tolerance of these mice. Nevertheless, the general phenotypic characteristics of these mice (weight, food intake, fasting glucose, and insulin levels) were not significantly different from the Itgβ1 littermate control or C57Bl/6 wild type mice. Although we do not know the basis for this difference, the studies by Schwander *et al.* (7) used Cre-recombinase driven by the human α-skeletal actin promoter in ARC/S or B6D2 mice. In contrast, we used muscle creatine kinase promoter driving Cre-recombinase in C57Bl/6 mice. Thus, it is possible that these differences may reflect either the degree of gene knock-out between the different Cre-recombinases or are due to differences in background strains.

In any case, we observed that the glucose infusion rate needed to maintain euglycemia in MCKItgβ1 KO mice was markedly less than that in the Itgβ1 control mice. These results provide evidence that whole body insulin resistance and perturbed glucose uptake are present in MCKItgβ1 KO mice. Furthermore, we found that whole body glucose turnover was significantly decreased in MCKItgβ1 KO mice during EU clamps. Moreover, the

FIGURE 11. **Loss of skeletal muscle β1 integrin receptor subunit expression results in an inhibition of Akt phosphorylation.** *A*, control Itgβ1$^{flox/flox}$ and MCKItgβ1 KO mice were given an intraperitoneal injection of either isotonic saline or insulin (1 units/kg). Ten minutes later the gastrocnemius skeletal muscle was isolated, and tissue extracts were prepared. The extracts were then subjected to immunoblotting with specific phosphoserine 473, phosphothreonine 308, and total Akt antibodies. *B*, quantification of the relative extent of insulin-stimulated Akt phosphorylation was determined from the average of 6–10 independent experiments. *, $p < 0.05$. *C*, the relative levels total ILK, GLUT4, Akt, and phosphoserine 473 Akt (*p-Akt S473*) was determined in duplicate for the control Itgβ1$^{flox/flox}$ and MCKItgβ1 KO mice at the end of the EU clamps.
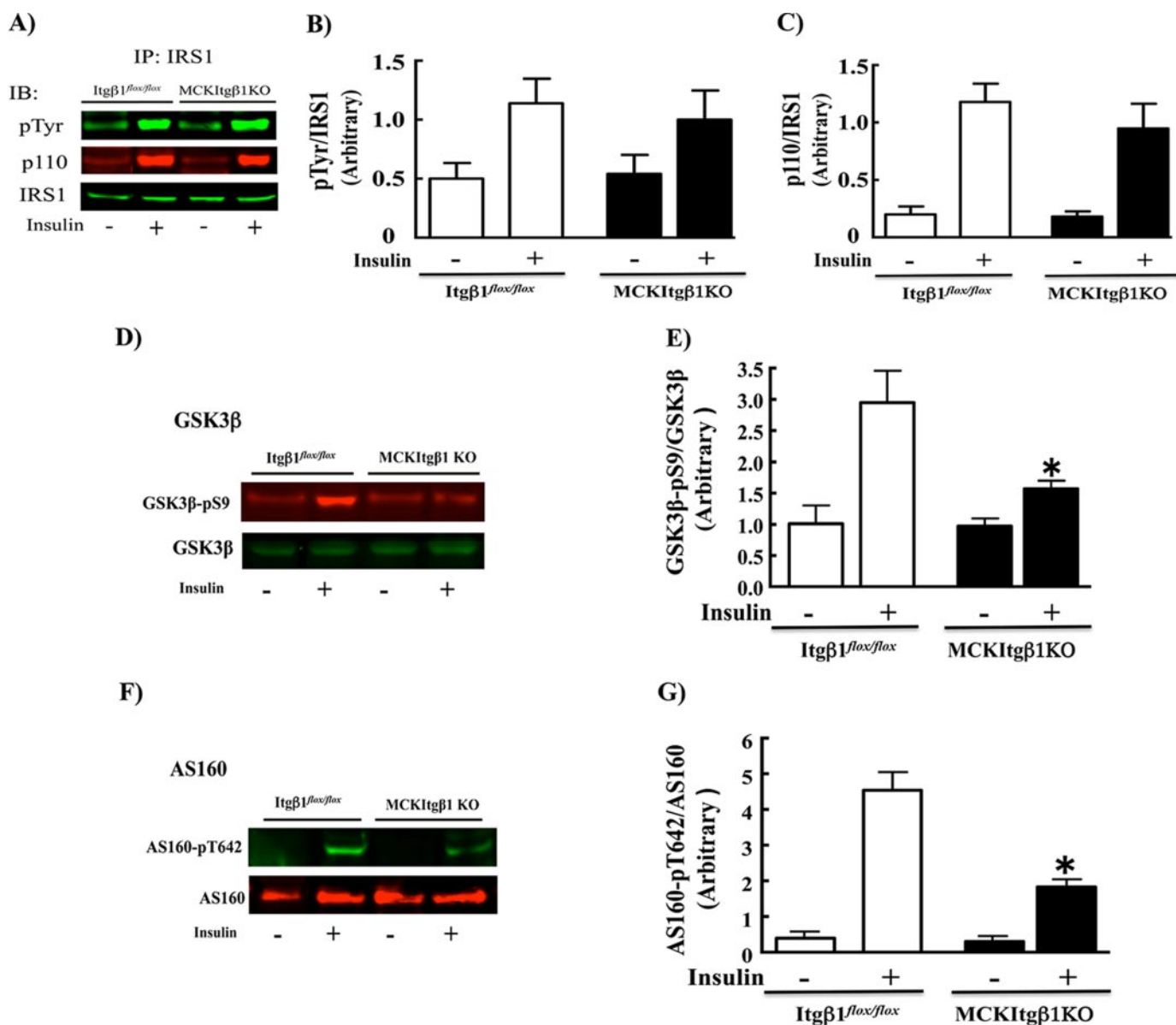
FIGURE 12. **MCKItgβ1 KO mice display normal insulin-stimulated IRS1 tyrosine phosphorylation and IRS1-associated PI 3-kinase but have defective downstream Akt signaling.** *A*, Itgβ1$^{flox/flox}$ and littermate MCKItgβ1 KO mice were injected with insulin (1 units/kg) for 10 min, and the gastrocnemius skeletal muscle was extracted and immunoprecipitate with an IRS1 antibody. The resultant immunoprecipitated was then immunoblotted (*IB*) with a phosphotyrosine (*pTyr*), the p110 PI 3-kinase catalytic subunit (*p110*), and IRS1 antibodies. *B*, quantification of the relative amount of phosphotyrosine labeled IRS1 compared with total amount of IRS1 was determined from three independent experiments. *C*, quantification of the relative amount of p110 co-precipitated with IRS1 compared with total amount of immunoprecipitated IRS1 was determined from three independent experiments. *D*, the gastrocnemius skeletal muscle extracts were immunoblotted for the presence of GSK3β serine 9 phosphorylation and total GSK3β. *E*, quantification of the relative amount of GSK3β-pS9 compared with total amount of GSK3β was determined from three independent experiments. *, $p < 0.02$. *F*, the gastrocnemius skeletal muscle extracts were immunoblotted for the presence of AS160 threonine 642 phosphorylation (*AS160-pT642*) and total GSK3β. *G*, quantification of the relative amount of AS160-pT642 compared with total amount of AS160 was determined from three independent experiments. *$p < 0.01$.

observed whole body insulin resistance was a direct result of impaired insulin-stimulated glucose uptake and glycogen synthesis in skeletal muscle but with apparent normal insulin signaling in the liver and adipose tissue. This result is also consistent with a recent study in cultured L6 myocytes indicating that a loss of focal adhesion kinase function, which is a downstream target of integrin β1, correlated with a reduction in insulin-stimulated glucose uptake, GLUT4 translocation to the plasma membrane, and glycogen synthesis (12). Interestingly, despite the decrease in skeletal muscle insulin sensitivity, the MCK-Itgβ1 KO mice had normal body weight and adiposity, probably

reflecting metabolic compensation as has been reported for the selective skeletal muscle insulin resistance GLUT4 and caveolin 3 knock-out mice (58–60).

To elucidate the molecular mechanisms behind the observed abnormalities in insulin stimulation of glucose transport and glycogen synthesis, we investigated the protein expression levels of several key insulin responsive proteins in the MCKItgβ1 KO mice. It is generally accepted that insulin-stimulated glucose uptake and glycogen synthesis requires a signaling cascade involving the activation of the type IA PI 3-kinase resulting in the phosphorylation and activation of Akt (38, 42). The activa-
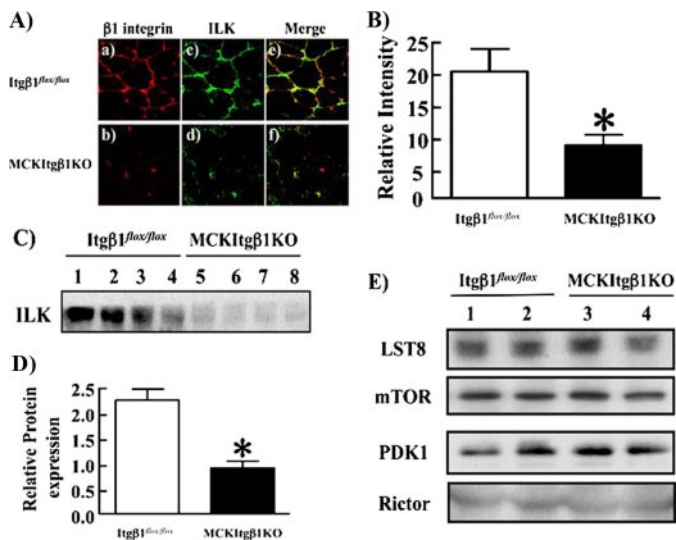
FIGURE 13. **Loss of β1 integrin receptor subunit expression results in a concomitant reduction in ILK expression without significant effect on the mTORC2 complex.** *A,* skeletal muscle (gastrocnemius) was isolated from 14-week-old Itgβ1*flox/flox* and littermate MCKItgβ1 KO mice. Sections were subjected to confocal immunofluorescence microscopy for the presence of β1 integrin subunit (*panels a* and *b*) and ILK (*panels c* and *d*). The merged images are shown in *panels e* and *f*. *B,* quantification of the decrease in ILK was determined by relative fluorescent intensity as described under "Experimental Procedures." *C,* the relative levels of ILK protein levels in gastrocnemius skeletal muscle from Itgβ1*flox/flox* and littermate MCKItgβ1 KO mice were determined by immunoblotting of representative samples in quadruplicate. *D,* quantification of the ILK protein levels was determined from the average of 6–10 independent experiments. *E,* the relative protein levels of LST8, mTOR, PDK1, and Rictor were determined by immunoblotting of representative samples in duplicate.

tion of Akt/protein kinase B requires its PH domain but also is dependent on phosphorylation of Thr-308 and Ser-473 (61). Phosphoinositide-dependent protein kinase 1 is responsible for threonine 308 phosphorylation (62, 63). However, the identity of PDK2 or the hydrophobic-motif kinase, responsible for Ser-473 phosphorylation, remains elusive (64). Although several potential PDK2 candidates have been suggested, recent data has implicated the mTOR·Rictor·LST8 complex as the upstream Akt Ser-473 kinase (22, 65). Additionally, earlier studies using both small interfering RNA-mediated gene silencing and conditional gene knockouts suggested that ILK also functions as an Akt Ser-473 kinase (19). Whether mTOR·Rictor·LST8 is the only *bona fide* hydrophobic motif kinase or other kinases can also serve this function under specific circumstances remains to be determined. In this regard, a conditional ILK knock-out in skeletal muscle has recently been found to impair exercise stimulated phosphorylation of Akt (66).

In either case our data clearly demonstrate that the loss of integrin β1 results in a marked impairment in Akt phosphorylation on Ser-473 concomitant with a reduction in ILK expression with no effect on Thr-308 phosphorylation. Because the protein levels of the mTORC2 complex (mTOR·Rictor·LST8) were unaffected, this suggests that in skeletal muscle ILK may serve as a primary insulin-dependent PDK2 kinase. Furthermore, the inhibition of insulin-stimulated Ser-473 Akt phosphorylation can thereby account for the impairment of insulin-stimulated glucose uptake in the MCKItgβ1 KO mice despite relatively normal levels of GLUT4 protein expression.

Although the concomitant reduction in ILK does not directly address whether or not ILK is the upstream kinase responsible for Akt Ser-473 phosphorylation, it does demonstrate that ILK expression is dependent upon the appropriate assembly of integrin β1 signaling complex organization *in vivo*. In summary, our data demonstrate an important requirement for integrin β1 subunit receptor signaling in modulating skeletal muscle insulin action and glucose homeostasis.

REFERENCES
1. Humphries, M. J. (2000) *Biochem. Soc. Trans.* **28,** 311–339
2. Clemmons, D. R., and Maile, L. A. (2005) *Mol. Endocrinol.* **19,** 1–11
3. Akiyama, S. K. (1996) *Hum. Cell* **9,** 181–186
4. Kuppuswamy, D. (2002) *Circ. Res.* **90,** 1240–1242
5. Giancotti, F. G., and Ruoslahti, E. (1999) *Science* **285,** 1028–1032
6. Schwander, M., Shirasaki, R., Pfaff, S. L., and Muller, U. (2004) *J. Neurosci.* **24,** 8181–8191
7. Schwander, M., Leu, M., Stumm, M., Dorchies, O. M., Ruegg, U. T., Schittny, J., and Muller, U. (2003) *Dev. Cell* **4,** 673–685
8. Guilherme, A., and Czech, M. P. (1998) *J. Biol. Chem.* **273,** 33119–33122
9. King, W. G., Mattaliano, M. D., Chan, T. O., Tsichlis, P. N., and Brugge, J. S. (1997) *Mol. Cell. Biol.* **17,** 4406–4418
10. Yujiri, T., Nawata, R., Takahashi, T., Sato, Y., Tanizawa, Y., Kitamura, T., and Oka, Y. (2003) *J. Biol. Chem.* **278,** 3846–3851
11. Delcommenne, M., Tan, C., Gray, V., Rue, L., Woodgett, J., and Dedhar, S. (1998) *Proc. Natl. Acad. Sci. U. S. A.* **95,** 11211–11216
12. Huang, D., Khoe, M., Ilic, D., and Bryer-Ash, M. (2006) *Endocrinology* **147,** 3333–3343
13. Huang, D., Cheung, A. T., Parsons, J. T., and Bryer-Ash, M. (2002) *J. Biol. Chem.* **277,** 18151–18160
14. Hannigan, G. E., Leung-Hagesteijn, C., Fitz-Gibbon, L., Coppolino, M. G., Radeva, G., Filmus, J., Bell, J. C., and Dedhar, S. (1996) *Nature* **379,** 91–96
15. Li, F., Zhang, Y., and Wu, C. (1999) *J. Cell Sci.* **112,** 4589–4599
16. Pasquet, J. M., Noury, M., and Nurden, A. T. (2002) *Thromb. Haemostasis* **88,** 115–122
17. Yamaji, S., Suzuki, A., Kanamori, H., Mishima, W., Takabayashi, M., Fujimaki, K., Tomita, N., Fujisawa, S., Ohno, S., and Ishigatsubo, Y. (2002) *Biochem. Biophys. Res. Commun.* **297,** 1324–1331
18. Yamaji, S., Suzuki, A., Sugiyama, Y., Koide, Y., Yoshida, M., Kanamori, H., Mohri, H., Ohno, S., and Ishigatsubo, Y. (2001) *J. Cell Biol.* **153,** 1251–1264
19. Troussard, A. A., Mawji, N. M., Ong, C., Mui, A., St-Arnaud, R., and Dedhar, S. (2003) *J. Biol. Chem.* **278,** 22374–22378
20. Pearce, L. R., Huang, X., Boudeau, J., Pawlowski, R., Wullschleger, S., Deak, M., Ibrahim, A. F., Gourlay, R., Magnuson, M. A., and Alessi, D. R. (2007) *Biochem. J.* **405,** 513–522
21. Wullschleger, S., Loewith, R., and Hall, M. N. (2006) *Cell* **124,** 471–484
22. Sarbassov, D. D., Guertin, D. A., Ali, S. M., and Sabatini, D. M. (2005) *Science* **307,** 1098–1101
23. Scheid, M. P., Marignani, P. A., and Woodgett, J. R. (2002) *Mol. Cell. Biol.* **22,** 6247–6260
24. Dormond, O., Madsen, J. C., and Briscoe, D. M. (2007) *J. Biol. Chem.* **282,** 23679–23686
25. Zierath, J. R., Krook, A., and Wallberg-Henriksson, H. (1998) *Mol. Cell. Biochem.* **182,** 153–160
26. Bjornholm, M., Kawano, Y., Lehtihet, M., and Zierath, J. R. (1997) *Diabetes* **46,** 524–527
27. Caro, J. F., Sinha, M. K., Raju, S. M., Ittoop, O., Pories, W. J., Flickinger, E. G., Meelheim, D., and Dohm, G. L. (1987) *J. Clin. Investig.* **79,** 1330–1337
28. Goodyear, L. J., Giorgino, F., Sherman, L. A., Carey, J., Smith, R. J., and Dohm, G. L. (1995) *J. Clin. Investig.* **95,** 2195–2204

29. Cusi, K., Maezono, K., Osman, A., Pendergrass, M., Patti, M. E., Pratipana-watr, T., DeFronzo, R. A., Kahn, C. R., and Mandarino, L. J. (2000) *J. Clin. Investig.* **105,** 311–320

30. Mandarino, L. J., Consoli, A., Jain, A., and Kelley, D. E. (1996) *Am. J. Physiol.* **270,** E463–E470

31. Damsbo, P., Vaag, A., Hother-Nielsen, O., and Beck-Nielsen, H. (1991) *Diabetologia* **34,** 239–245

32. Johnson, A. B., Argyraki, M., Thow, J. C., Jones, I. R., Broughton, D., Miller, M., and Taylor, R. (1991) *Metabolism* **40,** 252–260

33. Kim, Y. B., Nikoulina, S. E., Ciaraldi, T. P., Henry, R. R., and Kahn, B. B. (1999) *J. Clin. Investig.* **104,** 733–741

34. Potocnik, A. J., Brakebusch, C., and Fassler, R. (2000) *Immunity* **12,** 653–663

35. Bruning, J. C., Michael, M. D., Winnay, J. N., Hayashi, T., Horsch, D., Accili, D., Goodyear, L. J., and Kahn, C. R. (1998) *Mol. Cell* **2,** 559–569

36. Kanagawa, M., Michele, D. E., Satz, J. S., Barresi, R., Kusano, H., Sasaki, T., Timpl, R., Henry, M. D., and Campbell, K. P. (2005) *FEBS Lett.* **579,** 4792–4796

37. Kim, J. K., Wi, J. K., and Youn, J. H. (1996) *Diabetes* **45,** 651–658

38. Ohshima, K., Shargill, N. S., Chan, T. M., and Bray, G. A. (1984) *Am. J. Physiol.* **246,** E193–E197

39. Koch, L. G., and Britton, S. L. (2001) *Physiol. Genomics* **5,** 45–52

40. Nieswandt, B., Brakebusch, C., Bergmeier, W., Schulte, V., Bouvard, D., Mokhtari-Nejad, R., Lindhout, T., Heemskerk, J. W., Zirngibl, H., and Fassler, R. (2001) *EMBO J.* **20,** 2120–2130

41. Brakebusch, C., Grose, R., Quondamatteo, F., Ramirez, A., Jorcano, J. L., Pirro, A., Svensson, M., Herken, R., Sasaki, T., Timpl, R., Werner, S., and Fassler, R. (2000) *EMBO J.* **19,** 3990–4003

42. Watson, R. T., Kanzaki, M., and Pessin, J. E. (2004) *Endocr. Rev.* **25,** 177–204

43. Kanzaki, M. (2006) *Endocr. J.* **53,** 267–293

44. Tomas, E., Lin, Y. S., Dagher, Z., Saha, A., Luo, Z., Ido, Y., and Ruderman, N. B. (2002) *Ann. N. Y. Acad. Sci.* **967,** 43–51

45. Ryder, J. W., Gilbert, M., and Zierath, J. R. (2001) *Front. Biosci.* **6,** 154–163

46. Carvalho, E., Jansson, P. A., Nagaev, I., Wenthzel, A. M., and Smith, U. (2001) *FASEB J.* **15,** 1101–1103

47. Shulman, G. I. (2000) *J. Clin. Investig.* **106,** 171–176

48. Pencek, R. R., Bertoldo, A., Price, J., Kelley, C., Cobelli, C., and Kelley, D. E. (2006) *Am. J. Physiol. Endocrinol. Metab.* **290,** 1124–1130

49. Ginsberg, M. H., Wencel, J. D., White, J. G., and Plow, E. F. (1983) *J. Cell Biol.* **97,** 571–573

50. Kim, Y. B., Kotani, K., Ciaraldi, T. P., Henry, R. R., and Kahn, B. B. (2003) *Diabetes* **52,** 1935–1942

51. Karlsson, H. K., Zierath, J. R., Kane, S., Krook, A., Lienhard, G. E., and Wallberg-Henriksson, H. (2005) *Diabetes* **54,** 1692–1697

52. Joy, A. M., Beaudry, C. E., Tran, N. L., Ponce, F. A., Holz, D. R., Demuth, T., and Berens, M. E. (2003) *J. Cell Sci.* **116,** 4409–4417

53. Gary, D. S., and Mattson, M. P. (2001) *J. Neurochem.* **76,** 1485–1496

54. Gauthier, R., Harnois, C., Drolet, J. F., Reed, J. C., Vezina, A., and Vachon, P. H. (2001) *Am. J. Physiol. Cell Physiol.* **280,** 1540–1554

55. Tai, Y. T., Podar, K., Catley, L., Tseng, Y. H., Akiyama, M., Shringarpure, R., Burger, R., Hideshima, T., Chauhan, D., Mitsiades, N., Richardson, P., Munshi, N. C., Kahn, C. R., Mitsiades, C., and Anderson, K. C. (2003) *Cancer Res.* **63,** 5850–5858

56. Shai, S. Y., Harpf, A. E., Babbitt, C. J., Jordan, M. C., Fishbein, M. C., Chen, J., Omura, M., Leil, T. A., Becker, K. D., Jiang, M., Smith, D. J., Cherry, S. R., Loftus, J. C., and Ross, R. S. (2002) *Circ. Res.* **90,** 458–464

57. Shai, S. Y., Harpf, A. E., and Ross, R. S. (2002) *Genet. Eng.* **24,** 87–105

58. Zisman, A., Peroni, O. D., Abel, E. D., Michael, M. D., Mauvais-Jarvis, F., Lowell, B. B., Wojtaszewski, J. F., Hirshman, M. F., Virkamaki, A., Goodyear, L. J., Kahn, C. R., and Kahn, B. B. (2000) *Nat. Med.* **6,** 924–928

59. Oshikawa, J., Otsu, K., Toya, Y., Tsunematsu, T., Hankins, R., Kawabe, J., Minamisawa, S., Umemura, S., Hagiwara, Y., and Ishikawa, Y. (2004) *Proc. Natl. Acad. Sci. U. S. A.* **101,** 12670–12675

60. Kim, Y. B., Peroni, O. D., Aschenbach, W. G., Minokoshi, Y., Kotani, K., Zisman, A., Kahn, C. R., Goodyear, L. J., and Kahn, B. B. (2005) *Mol. Cell. Biol.* **25,** 9713–9723

61. Ren, J., Lew, S., Wang, Z., and London, E. (1997) *Biochemistry* **36,** 10213–10220

62. Stephens, L., Anderson, K., Stokoe, D., Erdjument-Bromage, H., Painter, G. F., Holmes, A. B., Gaffney, P. R., Reese, C. B., McCormick, F., Tempst, P., Coadwell, J., and Hawkins, P. T. (1998) *Science* **279,** 710–714

63. Alessi, D. R., James, S. R., Downes, C. P., Holmes, A. B., Gaffney, P. R., Reese, C. B., and Cohen, P. (1997) *Curr. Biol.* **7,** 261–269

64. Vanhaesebroeck, B., and Alessi, D. R. (2000) *Biochem. J.* **346,** 561–576

65. Hresko, R. C., and Mueckler, M. (2005) *J. Biol. Chem.* **280,** 40406–40416

66. Wang, H. V., Chang, L. W., Brixius, K., Wickström, S. A., Montanez, E., Thievessen, I., Schwander, M., Müller, U., Bloch, W., Mayer, U., and Fässler, R. (2008) *J. Cell Biol.* **180,** 1037–1049